

White dwarfs with infrared excess within 100 pc: *Gaia* and the Virtual Observatory

Murillo-Ojeda, R.¹, Jiménez-Esteban, F.¹, Rebassa-Mansergas, A.^{2,3},
Torres, S.^{2,3}, and Solano, E.¹

¹ Centro de Astrobiología (CAB), CSIC-INTA, Camino Bajo del Castillo s/n, campus ESAC, 28692, Villanueva de la Cañada, Madrid, Spain

² Departament de Física, Universitat Politècnica de Catalunya, c/Esteve Terrades 5, 08860 Castelldefels, Spain

³ Institute for Space Studies of Catalonia (IEEC), c/Esteve Terradas, 1, Edifici RDIT, Despatx 212, Campus del Baix Llobregat UPC – Parc Mediterrani de la Tecnologia, 08860 Castelldefels, Spain

Abstract

The infrared excess shown by white dwarfs can be an indicator of a low-mass substellar companion, like a brown dwarf or even an exoplanet. In this work, we describe the methodology followed to identify white dwarfs with infrared excess within 100 pc and we show the preliminary results. Our initial sample is an almost complete volume-limited white dwarf sample within 100pc. We use the available infrared photometry at the Virtual Observatory (VO) and the J-PAS synthetic photometry obtained from the *Gaia* DR3 spectra. This work may also be considered as the starting point of a spectroscopic study to unveil the nature of peculiar white dwarf systems.

1 Introduction

White dwarfs are stellar remnants of low and intermediate mass stars ($M < 8M_{\odot}$) [2]. The majority of stars formed in the Galaxy fall within this mass range, so the percentage of stars that end as white dwarfs is over 97%. Therefore, white dwarfs are one of the most common objects in the Galaxy. This is the reason why the study of white dwarfs is highly significant for our understanding of the Galaxy.

The latest *Gaia* data release, *Gaia* DR3, presented 200 million low resolution ($R \approx 60$) spectra [9]. These include around 100 000 white dwarfs [17]. These *Gaia* spectra cover from the ultraviolet to the near-infrared wavelength range (330 – 1050 nm).

The presence of infrared excess at white dwarf spectra can be related to the existence

of circumstellar material, like a debris disc, or a companion object, like a red dwarf star, a brown dwarf, or even an exoplanet. The study of these objects is crucial for understanding the presence of planetary systems around post main sequence environments.

2 Photometry search

We selected the volume-limited white dwarf sample within 100 pc built from *Gaia* DR3 spectra by Jimenez-Esteban et al. (2023) [12]. Their spectral classification was based on the atmosphere composition: hydrogen-rich (DA) and non-hydrogen-rich (non-DA). We refer the read to the original work for further details. Our initial sample was constituted by the 8 150 white dwarfs with a reliable spectral classification.

We built the optical photometry from the spectroscopic coefficients of *Gaia* DR3 [7]. We used the Python package *GaiaXPy*¹ to generate the synthetic photometry of Javalambre Physics of the Accelerating Universe Astronomical Survey (J-PAS²; [16, 4]). The J-PAS filter system is formed by 54 narrow filters (3780–9100 Å), 2 wider filters in the reddest and bluest part of the wavelength range, and 4 SDSS-like filters. This filter system was chosen because it has similar resolution and wavelength range to *Gaia* spectra.

In order to ensure the quality of the synthetic J-PAS data, we imposed two conditions: skip any J-PAS filter bluer than 4000 Å due to the low signal-to-noise ratio of *Gaia* spectra [10]; and a J-PAS flux relative error smaller than 10 %.

In order to identify infrared flux excesses, we required photometry at the infrared wavelengths. So, we queried at the following infrared surveys available through the Virtual Observatory (VO) using Topcat [22]:

- Two Micron All Sky Survey (2MASS, [21]): 2MASS All-Sky Catalog of point sources (PSC).
- Wide-field Infrared Survey Explorer (WISE, [24]): CatWISE2020 [18].
- UKIRT Infrared Deep Sky Survey (UKIDSS, [11]): Large Area Survey (LAS) DR10, Galactic Clusters Survey (GCS) DR10, Galactic Plane Survey (GPS) DR7, Ultra Deep Survey (UDS) DR10, Deep Extragalactic Survey (DXS) DR10.
- Visible and Infrared Survey Telescope for Astronomy (VISTA, [8]): VISTA Variables in the Via Lactea (VVV) DR5, VISTA Kilo-Degree Infrared Galaxy (VIKING) DR4, VISTA Hemisphere Survey (VHS) DR6, VISTA Deep Extragalactic Observations (VIDEO) DR5, VISTA Magellanic Survey (VMS) DR4.
- Spitzer [23]: The Spitzer Enhanced Imaging Products (SEIP) source list, Galactic Legacy Infrared Midplane Survey Extraordinaire (GLIMPSE) I, II & 3D.

¹<https://gaia-dpci.github.io/GaiaXPy-website/>

²<http://www.j-pas.org/>

The search was done by selecting a radius of $3''$ at the white dwarf position for each catalogue observing epoch. We selected white dwarfs with at least three reliable infrared photometric data with good quality flags. Detailed information of these catalogue’s filters can be found using the SVO Filter Profile Service³ [20].

3 Infrared excess detection

We used a similar methodology than in Rebassa-Mansergas et al. (2019) [19]. With the help of the Virtual Observatory SED Analyser (VOSA⁴, [3]), we analysed the spectral energy distribution (SED) of each white dwarf built with the collected optical and infrared photometry.

We used Koester atmospheric models [13] for DA (hydrogen pure) or DB (helium pure), accordingly with the spectral classification by Jimenez-Esteban et al. (2023) [12] catalogue to make a single body fit to the SEDs. Then, we looked for the SEDs with infrared excess emission with respect to the estimated flux by the model taking advantage of the automatic detection of VOSA. We selected the 739 white dwarfs showing infrared excess at least at two photometric data points as initial candidates. Figure 1 shows two examples of white dwarf SEDs with infrared excess emission.

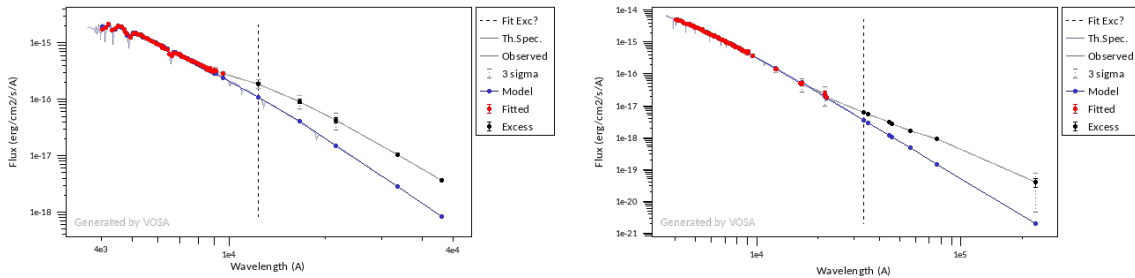


Figure 1: Single object SED fits, illustrating examples of white dwarfs with infrared excess emission. The red and black filled circles show the observed photometry, the black ones have flux excess with respect to the model shown in blue. The best-fitting model is Koester DA with $T_{\text{eff}} = 10\,250$ K (left-hand panel) and Koester DB with $T_{\text{eff}} = 14\,500$ K (right-hand panel).

Subsequently, we checked whether the infrared excess was due to contamination of near objects. We did a visual inspection of optical and infrared images available within the VO using Aladin⁵ [5], an interactive atlas of the sky. This was the most meticulous step of our methodology in order to obtain a reliable white dwarf with infrared excess catalogue. Figure 2 shows an example of contaminated white dwarf SED. We obtained a total of ~ 200 white dwarfs without contamination.

³<http://svo2.cab.inta-csic.es/theory/fps/>

⁴<http://svo2.cab.inta-csic.es/theory/vosa>

⁵<https://aladin.u-strasbg.fr/>

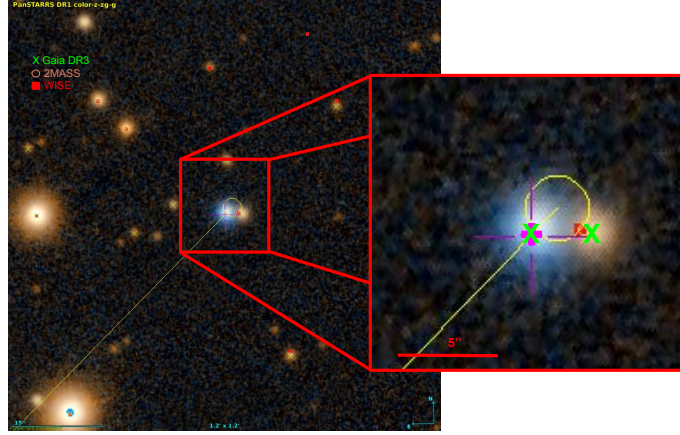


Figure 2: Example of contaminated white dwarf in an Aladin chart. The pink cross is on the white dwarf, the red square is the position of CatWISE, the green crosses are of Gaia DR3 and the orange circle is of 2MASS. The example shows how infrared photometry is placed on an angularly close object with different parallax.

Afterwards, we made a two-body fit to the SED in VOSA using the same Koester model as in the single fit for the white dwarf and either the BT-Settl (CIFIST) model grid [6, 1] or a black body emission curve for the second body, choosing the one that gave the best result. Figure 3 shows two examples of two-body SED fits.

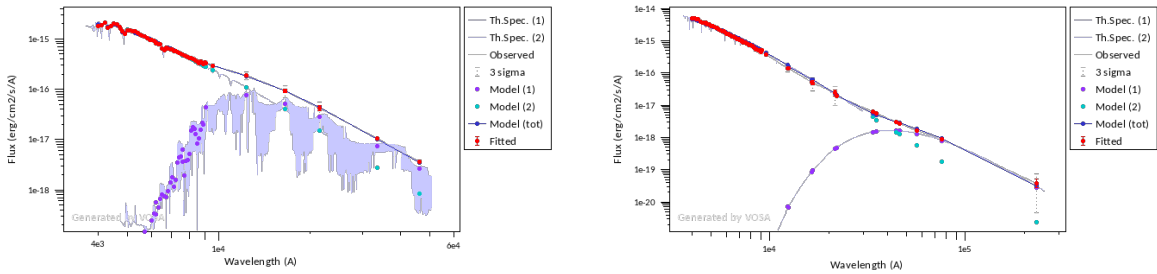


Figure 3: Two-body SED fits, illustrating the same examples of white dwarfs with infrared excess emission as in Fig. 1. The red filled circles show the observed photometry; the cyan circles show the Koester model and the purple ones the second body model. At the left-hand panel, the best models are Koester DA with $T_{\text{eff}} = 10\,250$ K and BT-Sett (CIFIST) with $T_{\text{eff}} = 2\,200$ K. At the right-hand panel, the best models are Koester DB with $T_{\text{eff}} = 12\,750$ K and Black Body with $T_{\text{eff}} = 700$ K.

4 Preliminary results and future work

Our preliminary results were ~ 200 white dwarfs with reliable infrared excess emission.

According to the spectral classification obtained for these white dwarfs there were $\sim 68\%$

DAs and $\sim 32\%$ non-DAs. Furthermore, if we looked at the second body fit, it was revealed that $\sim 75\%$ had a best BT-Settl (CIFIST) fit and $\sim 25\%$ had a best Black Body fit ($T_{\text{eff}} < 1200$ K). When we looked at the mass and the temperature distributions, we saw that mass distribution had the predicted peak at $0.6 M_{\odot}$ and at the temperature distribution a concentration of white dwarfs at the lowest temperatures, as it is showed at Figure 4. We have 53 objects in common with Rebassa-Mansergas et al. (2019) [19] sample. This work increased the number of white dwarfs with infrared excess within 100 pc by a factor of three compared to the previous sample. The difference between the samples is because of the new data available like *Gaia* DR3 synthetic photometry, CatWISE2020 or new infrared data releases; and taking into account the proper motion of the objects and a smaller search radius.

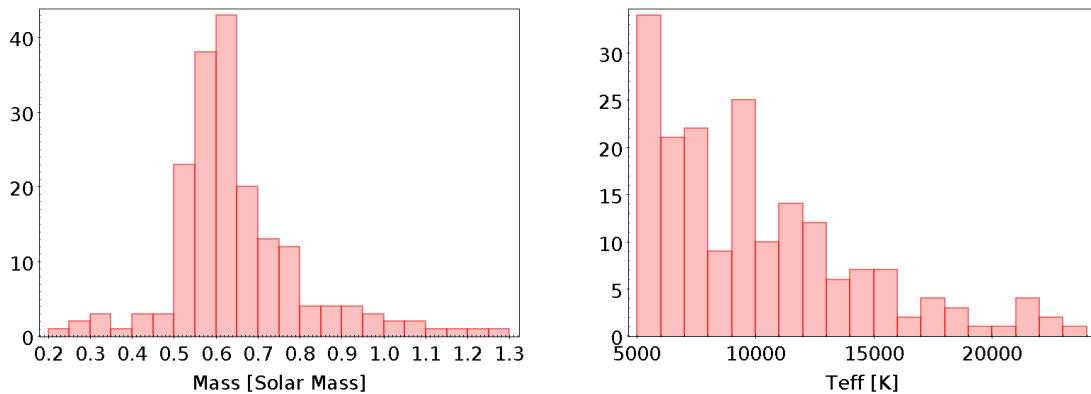


Figure 4: Preliminary mass (left-hand panel) and temperature (right-hand panel) diagrams.

It should be noted that these results are preliminary as we are in the process of verify the non-contaminated objects using *Aladin*. In the near future, we will publish the final results with the analysis and the comparison with other infrared excess white dwarf catalogues [19, 25, 14, 15]. As a future work, we will start a follow-up program of the most promising infrared candidates using ground-based telescopes, such as the Very Large Telescope or the Gran Telescopio CANARIAS, to determine the cause of the infrared excess.

Acknowledgments

Based on data from the SVO archive of White Dwarfs from *Gaia* at CAB (CSIC-INTA). This publication makes use of VOSA, developed under the Spanish Virtual Observatory project. VOSA has been partially updated by using funding from the European Union’s Horizon 2020 Research and Innovation Programme, under Grant Agreement n^o 776403 (EXOPLANETS-A). This research has made use of the SVO Filter Profile Service “Carlos Rodrigo”, funded by MCIN/AEI/10.13039/501100011033/through grant PID2020-112949GB-I00. This research has made use of TOPCAT [22]. This research has made use of “Aladin sky atlas” developed at CDS, Strasbourg Observatory, France. This research has made use of the SIMBAD and VizieR databases, operated by CDS at Strasbourg, France. This work has made use of data from the European Space Agency (ESA) mission *Gaia* (<https://www.cosmos.esa.int/gaia>), processed by the *Gaia* Data Processing and Analysis Consortium (DPAC, <https://www.cosmos.esa.int/web/gaia/dpac/consortium>). Funding for the DPAC

has been provided by national institutions, in particular the institutions participating in the *Gaia* Multilateral Agreement. This work has made use of the Python package GaiaXPY, developed and maintained by members of the *Gaia* Data Processing and Analysis Consortium (DPAC), and in particular, Coordination Unit 5 (CU5), and the Data Processing Centre located at the Institute of Astronomy, Cambridge, UK (DPCI).

This research has made use of the Spanish Virtual Observatory (<https://svo.cab.inta-csic.es>) project funded by the Spanish Ministry of Science and Innovation/State Agency of Research MCIN/AEI/10.13039/501100011033 through grant PID2020-112949GB-I00.

RMO is funded by INTA through grant PRE-OBSERVATORIO.

References

- [1] Allard, F., Homeier, D., & Freytag, B. 2012, *Philosophical Transactions of the Royal Society of London Series A*, 370, 2765
- [2] Althaus L. G., Córscico A. H., Isern J., & García-Berro E. 2010, *A&AR*, 18, 471
- [3] Bayo, A., Rodrigo, C., Barrado y Navascués, D., et al. 2008, *A&A*, 492, 277B
- [4] Benitez, N., Dupke, R., Moles, M., et al. 2014, arXiv:1403.5237
- [5] Bonnarel, F., Fernique, P., Bienaymé, O., et al. 2000, *A&AS*, 143, 33
- [6] Caffau, E., Ludwig, H. G., Steffen, M., Freytag, B. et al. 2011, *Sol. Phys.*, 268, 255
- [7] Carrasco, J. M., Weiler, M., Jordi, C., et al. 2021, *A&A*, 652, A86
- [8] Cross, N. J. G., Collins, R. S., Mann, R. G., et al. 2012, *A&A*, 548, A119
- [9] De Angeli, F., Weiler, M., Montegriffo, P., et al. 2023, *A&A*, 674, A2
- [10] Gaia Collaboration, Montegriffo, P., Bellazzini, M., et al. 2023, *A&A* 674, A33.
- [11] Hewett, P. C., Warren, S. J., Leggett, S. K., & Hodgkin, S. T. 2006, *MNRAS*, 367, 454
- [12] Jiménez-Esteban, F. M., Torres, S., Rebassa-Mansergas, A., et al. 2023, *MNRAS*, 518, 5106-5122
- [13] Koester D., 2010, *Mem. Soc. Astron. Ital.*, 81, 921
- [14] Lai, S., Dennihy, E., Xu, S., et al. 2021, *ApJ*, 920, 156
- [15] Madurga Favieres, C., Kissler-Patig, M., Xu, Siyi, X. et al. 2024, *A&A*, 688, A168
- [16] Marín-Franch, A., Chueca, S., Moles, M., et al. 2012, in *Modern Technologies in Space- and Ground-based Telescopes and Instrumentation II*, 8450, 84503S
- [17] Montegriffo, P., De Angeli, F., Andrae, R., et al. 2023, *A&A*, 674, A3
- [18] Marocco, F., Eisenhardt, P. R. M., Fowler, J. W., et al. 2021, *ApJS*, 253, 8
- [19] Rebassa-Mansergas, A., Solano, E., Xu, S., et al. 2019, *MNRAS*, 489, 3990-4000
- [20] Rodrigo, C., Cruz, P., Aguilar, J. F., et al. 2024, *A&A*, 689, A93
- [21] Skrutskie, M. F., Cutri, R. M., Stiening, R., et al. 2006, *AJ*, 131, 1163
- [22] Taylor, M. B. 2005, *ASP Conf. Ser.*, 347, 29
- [23] Werner, M. W., Roellig, T. L., Low, F. J., et al. 2004, *ApJS*, 154, 1
- [24] Wright, E. L., Eisenhardt, P. R. M., Mainzer, A. K., et al. 2010, *AJ*, 140, 1868
- [25] Xu, S., Lai, S., & Dennihy, E. 2020, *ApJ*, 902, 127